DMD Fast Forward. Published on December 1, 2020 as DOI: 10.1124/dmd.120.000136
This article has not been copyedited and formatted. The final version may differ from this version.

1. Title page:

Impact of direction of transport on the evaluation of inhibition potencies of multidrug and toxin extrusion protein 1 (MATE1) inhibitors

Asami Saito, Naoki Ishiguro, Masahito Takatani, Bojan Bister and Hiroyuki Kusuhara

Pharmacokinetics and Non-Clinical Safety Department, Nippon Boehringer Ingelheim Co., Ltd., Kobe, Japan (A.S., N.I, M.T., B.B); Laboratory of Molecular Pharmaceutics, Graduate School of Pharmaceutical Sciences, The University of Tokyo, Tokyo, Japan (H.K.)

DMD Fast Forward. Published on December 1, 2020 as DOI: 10.1124/dmd.120.000136
This article has not been copyedited and formatted. The final version may differ from this version.

2. Running title page:

a) Running title

Impact of transport direction on MATE1 inhibition

b) Corresponding author:

Prof. Hiroyuki Kusuhara

Laboratory of Molecular Pharmaceutics, Graduate School of Pharmaceutical Sciences, The University of Tokyo, 7-3-1, Hongo, Bunkyo-ku, Tokyo 113-0033, Japan

Phone: +81-3-5841-4774

Fax: +81-3-5841-4766

Email: kusuhara@mol.f.u-tokyo.ac.jp

c) Number of text pages: 27

Number of tables: 1

Number of figures: 4

Number of references: 30

Number of words (Abstract): 232

Number of words (Introduction): 571

Number of words (Discussion): 1434

d) **Abbreviations**:

DDI, drug-drug interaction;

HEK293, human embryonic kidney 293,

MATE, multidrug and toxin extrusion;

MPP^+, 1-methyl-4-phenylpyridinium;

DMD Fast Forward. Published on December 1, 2020 as DOI: 10.1124/dmd.120.000136
This article has not been copyedited and formatted. The final version may differ from this version.

3. Abstract

Multidrug and toxin extrusion (MATE) transporters are expressed on the luminal membrane of renal proximal tubule cells and extrude their substrates into the luminal side of the tubules. Inhibition of MATE1 can reduce renal secretory clearance of its substrate drugs, and lead to drug-drug interactions (DDI). In order to address if IC_{50} values of MATE1 inhibitors with regard to their extracellular concentrations are affected by the direction of MATE1-mediated transport, we established an efflux assay of 1-methyl-4-phenylpyridinium (MPP^+) and metformin using the HEK293 model transiently expressing human MATE1. The efflux rate was defined by reduction of the cellular amount of MPP^+ and metformin for 0.25 min shortly after the removal of extracellular MPP^+ and metformin. Inhibition potencies of 12 inhibitors towards MATE1-mediated transport were determined in both uptake and efflux assays. When MPP^+ was used as a substrate, 8 out of 12 inhibitors showed comparable IC_{50} values between assays (<4-fold). IC_{50} values from the efflux assays were higher for cimetidine (9.9-fold), trimethoprim (10-fold), famotidine (6.4-fold), and cephalexin (>3.8-fold). When metformin was used as a substrate, IC_{50} values of the tested inhibitors when evaluated using uptake and efflux assays were within 4-fold of each other, with an exception of cephalexin (>4.7-fold). IC_{50} values obtained from the uptake assay using metformin showed smaller IC_{50} values than those from efflux assay. Therefore, the uptake assay is recommended to determine IC_{50} values for the DDI predictions.

DMD Fast Forward. Published on December 1, 2020 as DOI: 10.1124/dmd.120.000136
This article has not been copyedited and formatted. The final version may differ from this version.

4. Significance statement

In this study, a new method to evaluate IC_{50} values of extracellular added inhibitors utilizing an efflux assay was established. IC_{50} values were not largely different between uptake and efflux directions but smaller in uptake. This study supports the rationale for commonly accepted uptake assay with metformin as an in vitro probe substrate for MATE1-mediated DDI risk assessment in drug development.

DMD Fast Forward. Published on December 1, 2020 as DOI: 10.1124/dmd.120.000136
This article has not been copyedited and formatted. The final version may differ from this version.

5. Introduction

The multidrug and toxic compound extrusion (MATE) family of transporters are ubiquitously expressed in organisms from several kingdoms of life, including Archaea, bacteria, and plants, and export cationic compounds using the H^+ or Na^+ gradient across plasma membranes. The human MATE orthologues MATE1 (SLC47A1) and MATE2-K (SLC47A2) are expressed on the brush border membrane of proximal tubule cells and work as organic cations/H^+ antiporters driven by an H^+ gradient (Yonezawa and Inui, 2011a; Motohashi and Inui, 2013). While 1-methyl-4-phenylpyridinium (MPP^+) and metformin are prototypical substrates of MATEs, extensive studies have identified various compounds as MATE1 and MATE2-K substrates, including endogenous metabolites such as creatinine (Terada and Inui, 2008). Quantitative targeted proteomics revealed abundant MATE1 expression in the human kidney cortex, while MATE2-K expression was detectable but below the lower limit of quantification (Prasad et al., 2016), suggesting that MATE1 is the major MATE isoform in the kidney. MATEs also play an important role in several clinical drug-drug interactions (DDIs) (Tsuda et al., 2009; Kusuhara et al., 2011; Ito et al., 2012), renal toxicities (Yonezawa and Inui, 2011b; Li et al., 2013), and drug efficacy (Becker et al., 2009; Stocker et al., 2013). MATE-mediated DDIs can result in a reduction in the renal clearance of co-administered drugs, or other compounds, that are MATE substrates (Ivanyuk et al., 2017). A reversible increase in levels of serum creatinine, a frequently used biomarker for kidney function, can occur by inhibiting its MATE-mediated tubular secretion (Chu et al., 2016; Nakada et al., 2019). Due to the emerging importance of MATE transporters in DDIs, regulatory authorities recently revised their guidelines for drug interaction studies to include MATEs. As such, sponsors now routinely evaluate the in vitro DDI potential of investigational compounds towards these transporters (US Food and Drug Administration (FDA), 2019;, Ministry of Health, Labor and Welfare (MHLW), 2018;, European Medicines Agency (EMA), 2012).

DMD Fast Forward. Published on December 1, 2020 as DOI: 10.1124/dmd.120.000136
This article has not been copyedited and formatted. The final version may differ from this version.

To profile compounds that interact with MATE transporters, the uptake of in vitro probe substrates into cells that overexpress a MATE transporter, defined in this paper as an "uptake assay" or "uptake direction", is one of the most commonly used methods. This methodology assumes that MATEs exhibit symmetric transport in both uptake and efflux directions. Considering the physiological role of MATEs as efflux transporters in the kidney, there are concerns about the impact of the direction of transport on IC_{50} values estimation. Several crystal structures of MATE orthologues have been reported (NorM-VC from *Vibrio cholerae*, DinF-BH from *Bacillus halodurans*, pfMATE from *Pyrococcus furiosus*, eMATE from *Arabidopsis thaliana*) (He et al., 2010; Lu et al., 2013; Tanaka et al., 2013; Miyauchi et al., 2017); however, most of the available structures to date focus on only outward facing portions of the protein and therefore symmetry of MATE transporters across cell membranes is not well understood. Whereas Dangprapai et al. revealed that the inward and outward facing MATE1 protein is symmetric by checking the kinetic interaction of H^+ with MATE1, no information regarding symmetric interaction substances other than H^+ is available (Dangprapai and Wright, 2011).

In this study, we developed the efflux assay to simply focus on the impact of the direction of transport toward IC_{50} determination, and compared the inhibition potency of 12 known MATE transporter inhibitors with regard to their extracellular concentrations for both uptake and efflux of two MATE1 substrates, MPP^+ and metformin, in MATE1-overexpressing cells. Furthermore, DDI predictions involving MATE1 were assessed using the $I_{max,u}/IC_{50}$ approach as currently recommended by regulatory agencies.

DMD Fast Forward. Published on December 1, 2020 as DOI: 10.1124/dmd.120.000136
This article has not been copyedited and formatted. The final version may differ from this version.

6. Materials and Methods

Chemicals and reagents

Unlabeled metformin was purchased from Wako Pure Chemical Industries (Osaka, Japan), and unlabeled 1-methyl-4-phenylpyridinium (MPP^+) was purchased from Sigma-Aldrich (St. Louis, MO, USA). [^{14}C]metformin (100 mCi/mmol) and [^{3}H]metformin (8 Ci/mmol) were purchased from Moravek Biochemicals (Brea, CA, USA), and [^{3}H]MPP^+ (80 Ci/mmol) was purchased from American Radiolabeled Chemicals (Saint Louis, MO, USA). All other chemicals and reagents were of analytical grade and are commercially available.

Cell culture and transfection

HEK293 cells transiently expressing human MATE1 were cultured in poly-D-lysine-coated 24-well plates as described in our previous study (Lechner et al., 2016). Culture medium supplemented with 5 mM sodium butyrate was added approximately 24 h after transfection to induce transporter gene expression. Uptake and efflux experiments were conducted approximately 48 h after transfection.

Uptake experiments using transiently transfected HEK293 cells

Cells were washed twice and incubated with transport buffer supplemented with 20 mM NH_4Cl for 10 min at 37°C. Medium was replaced with NH_4Cl-free transport buffer and cells were incubated for additional 5 min for intracellular pre-acidification. The composition of transport buffer was as follows: 130 mM KCl, 2 mM KH_2PO_4, 1.2 mM $MgSO_4$, 1 mM $CaCl_2$, 20 mM HEPES, and 5 mM glucose. Uptake was initiated by replacing buffer with transport buffer containing radiolabeled [^{3}H]MPP^+ or [^{14}C]metformin with or without inhibitors. Uptake was terminated at the designated incubation times by removal of drug solution followed by an addition of ice-cold transport buffer. The cells were then washed three times

DMD Fast Forward. Published on December 1, 2020 as DOI: 10.1124/dmd.120.000136
This article has not been copyedited and formatted. The final version may differ from this version.

with 0.5 ml of ice-cold transport buffer. Cells were solubilized with NaOH for 1 h at 37°C, and the lysate was neutralized by adding HCl. Aliquots of the cell lysates were transferred to scintillation vials containing scintillation cocktail (Ultima Gold XR; PerkinElmer Waltham, MA, USA) and radioactivity was measured in a liquid scintillation counter (TRI-CARB 3110TR, PerkinElmer, Waltham, MA, USA). The protein concentration was determined using the Lowry method with bovine serum albumin as the protein standard (Lowry et al., 1951).

Efflux experiments using transiently transfected HEK293 cells

Cells were washed twice and incubated with NH_4Cl-free transport buffer for 30 min at 37°C. Then medium was replaced with NH_4Cl-free transport buffer containing [^{3}H]MPP^+ or [^{3}H]metformin and incubated for an additional 10 min to pre-load the labelled substrate into the cells. Efflux was initiated by replacing pre-loading buffer with transport buffer supplemented with 20 mM NH_4Cl with and without inhibitors. Termination of efflux, cell lysis, radioactivity measurement, and determination of protein concentration were done as described in uptake experiments (Supplemental Figure 3). Total intracellular substrate concentration was determined assuming 6.5 μL as cellular volume per milligram protein (Gillen and Forbush, 1999).

Determination of intracellular pH

Intracellular pH was determined using a pH-sensitive fluorescent dye. HEK293 cells expressing MATE1 were pre-loaded with 2',7'-bis-(2-carboxyethyl)-5-(and-6)-carboxyfluorescein acetoxymetyl (BCECF-AM) at 37°C for 30 min. The fluorescence intensity (excitation at 488 nm and 460 nm, emission at 535 nm) was measured and the ratio of fluorescence from the two wavelengths monitored in a fluorescence plate reader (Enspire, PerkinElmer). Intracellular pH of MATE1-HEK293 cells

DMD Fast Forward. Published on December 1, 2020 as DOI: 10.1124/dmd.120.000136
This article has not been copyedited and formatted. The final version may differ from this version.

was calibrated using standardized pH buffers containing 10 μM nigericin (Thomas et al., 1979).

Data analysis

MATE1-mediated uptake clearance was calculated by normalizing the amount of radioactivity inside the cells to that in the buffer and the protein concentration in each well using the following equation:

$$Uptake\ CL = \frac{X_{cell}}{C_{buffer}}$$

where *Uptake CL* is the uptake clearance (μl/designated time point/mg), X_{cell} is the radioactivity in the cells (dpm/designated time/well), and C_{buffer} is the concentration of radioactivity in the buffer (dpm/μl). Uptake CL was normalized by the amount of total cellular protein (mg/well). MATE1-mediated uptake was calculated by subtracting the uptake into mock vector-transfected cells from that into MATE1-transfected cells.

MATE1-mediated efflux clearance was calculated by subtracting the remaining amount of substrate within the cells from that in the presence of 100 μM pyrimethamine, which was assumed to inhibit MATE1 completely, and normalized by AUC of intracellular substrate concentration-time curve and protein concentration in each well as following equation:

$$Efflux\ CL = \frac{X_{t_n,pyr} - X_{t_n}}{AUC_{0-t_n}}$$

where *Efflux CL* is the efflux clearance (μl/designated time/mg), $X_{t_n,pyr}$ is the radioactivity remained in the cells at t_n in the presence of 100 μM pyrimethamine (dpm/designated time/well), X_{t_n} is the radioactivity remained in the cells at t_n (dpm/designated time/well), *Efflux CL* was normalized by the amount of protein (mg/well).

DMD Fast Forward. Published on December 1, 2020 as DOI: 10.1124/dmd.120.000136
This article has not been copyedited and formatted. The final version may differ from this version.

Because the uptake of probe substrates during the pre-loading phase is largely different and it is difficult to use the identical initial intracellular concentration between MATE1-transfected cells and mock vector-transfected cells, MATE1-transfected cells incubated in presence of 100 μM pyrimethamine were used as control cells assuming no MATE1 activity.

Decrease of the total intracellular substrate concentration during efflux incubations was assumed to follow first-order elimination and the change of intracellular concentration over time was described by

$$AUC_{0-t_n} = \frac{t_n \times (C_0 - C_{t_n})}{\ln(C_0 / C_{t_n})}$$

where *AUC* is area under the total intracellular substrate concentration-time curve (μM×min), t_n is efflux incubation time (min), C_0 is the initial total intracellular substrate concentration (μM), and C_{t_n} (μM) is the total intracellular substrate concentration at t_n. t_n was set to 0.25 min as minimum feasible time.

The half-inhibitory concentrations (IC_{50}) of each inhibitor was determined using GraphPad PRISM software version 8.3.0 (GraphPad Software, San Diego, CA) based on the four – parameter logistic equation:

$$CL = CL_{min} + \left(\frac{(CL_{max} - CL_{min})}{1 + 10^{((logIC_{50} - I) \times Hill)}} \right)$$

where *CL* represents the uptake or efflux clearance, *I* is the concentration of inhibitor in the extracellular buffers, and *Hill* is the slope factor.

DMD Fast Forward. Published on December 1, 2020 as DOI: 10.1124/dmd.120.000136
This article has not been copyedited and formatted. The final version may differ from this version.

7. Results

Effect of NH_4CL on intracellular pH (pHi) to modulate the H^+ gradient

Acute exposure to NH_4Cl increased intracellular pH apparently to around pH 8.0 at all NH_4Cl concentrations (a pH greater than 8 could not be reliably determined due to a limitation of the method, Supplemental Figure 1). At 20 mM NH_4Cl, the intracellular pH was greater than 8.0 immediately after the medium change. It was maintained up to 10 min after the medium change and then gradually returned to basal pH (Supplemental Figure 2).

Washout of NH_4Cl by replacement with buffer lacking NH_4Cl decreased intracellular pH in a concentration-dependent manner. In our previous study, where 20 mM NH_4Cl was used for intracellular pre-acidification (Lechner et al., 2016), the intracellular pH in the uptake assay was around 6.5 and was maintained for several minutes, which is a sufficient duration as the incubation time was 1 min. Subsequently, 20 mM NH_4Cl was used in all experiments to generate an artificial pH gradient.

Time and concentration-dependent efflux of [^{3}H]MPP^+ and [^{3}H]metformin

MPP^+ and metformin were selected as probe substrates in this study because they are the most studied prototypical and/or clinical relevant organic cations for MATE assays. In addition, IC_{50} values towards MATE1 using these two substrates were comparable in uptake assays in previous studies (Lechner et al., 2016; Martinez-Guerrero et al., 2016).

The efflux of MPP^+ and metformin from MATE1-expressing cells or mock-vector transfected cells is shown in Figure 1. A time-dependent decrease of intracellular substrate concentration was only observed in MATE1-expressing cells, but not in control cells. The decrease of intracellular substrates was curve-linear in semi-log plots. In particular, this tendency was remarkable when MPP^+ was used (Figure 1). According to the preliminary experiment, it was not practical to determine IC_{50} values in shorter incubation time than 0.25

DMD Fast Forward. Published on December 1, 2020 as DOI: 10.1124/dmd.120.000136
This article has not been copyedited and formatted. The final version may differ from this version.

min due to the small change in the cellular amount of MPP^+ or metformin, resulting in a non-negligible experimental variability of the efflux rates. The subsequent analysis was conducted at 0.25 min as the minimum feasible incubation time in further assays for both probe substrates.

Efflux clearance of MPP^+ and metformin from MATE1-expressing cells decreased as shown by an increase of intracellular concentration of substrates (Supplemental Figure 4), resulting in apparent K_m values of 10-100 μM (MPP^+) and 100-1000 μM (metformin), respectively. The nominal concentrations of MPP^+ and metformin in pre-loading solutions were set at 0.05 and 0.75 μM, respectively, because the experimentally-determined total intracellular concentrations of the substrates used were 1 and 10 μM, which is similar to the substrate concentrations used in the inhibition study in the uptake direction (Lechner et al., 2016).

Comparison of uptake and efflux IC_{50} using MPP^+ and metformin as a substrate

Inhibition potencies of dolutegravir, vantedanib, cephalexin, ranolazine, lansoprazole and cobicistat, which are reported to cause clinical DDIs via inhibition of MATE1, were investigated in the uptake direction (Table 1, Supplemental Figure 5), along with the six compounds investigated previously (Lechner et al., 2016). Additionally, inhibition potencies of these 12 compounds were determined in the efflux direction. In both assays, IC_{50} values were defined by inhibitor concentrations in the buffer added to the outside of the cells (Table 1, Figure 2, 3, 4 and Supplemental Figure 5).

When MPP^+ was used as a substrate, differences in IC_{50} values between uptake and efflux mode were within 4-fold for 8 out of the 12 inhibitors. For cimetidine, trimethoprim, famotidine, and cephalexin, IC_{50} values were greater in efflux mode, showing 9.9-fold, 10-fold, 6.4-fold, and >3.8-fold differences when compared to the uptake mode, respectively

DMD Fast Forward. Published on December 1, 2020 as DOI: 10.1124/dmd.120.000136
This article has not been copyedited and formatted. The final version may differ from this version.

(Table 1 and Figure 4). When metformin was used as a substrate, all IC_{50} values, except for cephalexin, were within 4-fold between uptake and efflux directions (Table 1 and Figure 4).

DMD Fast Forward. Published on December 1, 2020 as DOI: 10.1124/dmd.120.000136
This article has not been copyedited and formatted. The final version may differ from this version.

8. Discussion

The most commonly used in vitro inhibition assay against MATE1 determines the inhibition potency of extracellularly added compounds by assessing the uptake of probe substrates into MATE1-expressing cells. Thus, this commonly used assay assumes IC_{50} values are identical and independent from whichever direction the substrates are transported. In order to address if DDI risk predictions based on regulatory guidelines are different or not depending on the direction of transport, IC_{50} values of various MATE1 inhibitors were generated in "uptake mode" and "efflux mode" based on their extracellular concentrations.

To achieve this, we developed an efflux inhibition assay for MATE1 after pre-loading two different substrates, MPP^+ and metformin, into MATE1-overexpressing cells. Initially, we aimed to measure the amount of substrate being effluxed into the medium. However, due to carry over from the pre-loading solution and loss of substrate from the cells during necessary subsequent washing steps, efflux clearance was determined based on the time-concentration profiles of remaining substrate within the cells (Figure 1). The time-dependent decrease in the cells suggested at least two rate constants, one fast and the other much slower in both substrates. And this phenomena was more obvious especially to MPP^+. Organic cations are distributed into acidic subcellular compartments such as endosomes (Martínez-Guerrero et al., 2016), which is referred to as endosomal trapping. According to Martinez-Guerrero, substrate release from endosomes was slow, and the rate constant for initial efflux of MPP^+ from MATE1-CHO cells was not changed regardless of the disruption of endosomal trapping by the addition of V type H^+-ATPase inhibitor. Therefore, assuming that the fast phase represents the efflux from the shallow compartment of the cells, we set 0.25 min as a minimum feasible incubation time for further efflux assay. As a preliminary experiment, we examined the dependence of the efflux clearance on the pre-loaded substrate concentrations (Supplemental Figure 4). The efflux clearance was

DMD Fast Forward. Published on December 1, 2020 as DOI: 10.1124/dmd.120.000136
This article has not been copyedited and formatted. The final version may differ from this version.

decreased along with an increase in the intracellular concentration, presumably due to the saturation of MATE1-mediated efflux. Apparent K_m values for MPP^+ and metformin were estimated in the rage of 10-100 μM and 100-1000 μM , respectively, which were not largely different from reported K_m values of MATE1-mediated MPP^+ and metformin in the uptake direction (47.6 μM and 208 μM, respectively) (Lechner et al., 2016). Approximation accuracy of these apparent K_m for the true K_m depends on the intracellular unbound fraction.

This study examined the direction- and substrate-dependency of IC_{50} values for the MATE1 substrates MPP^+ and metformin by comparing IC_{50} values obtained in uptake and efflux mode (Figure 4A), and by comparing IC_{50} values between MPP^+ and metformin (Figure 4B). Regarding direction-dependent inhibition, differences in IC_{50} values for 8 out of 12 compounds were within 4-fold when comparing uptake and efflux mode when MPP^+ was used as the probe substrate, although IC_{50} values for cimetidine, trimethoprim, famotidine, and cephalexin differed by greater than 4-fold (Figure 4A). When metformin was used as the probe substrate, the difference in IC_{50} values between uptake and efflux mode were within 4-fold difference for every inhibitor tested except cephalexin, which showed very weak inhibition in both assays (Figure 4A). Regarding substrate-dependency, all 12 compounds showed almost identical IC_{50} values (<2.3-fold) for both substrates in uptake assays. Our results are therefore consistent with previously reported substrate-independent IC_{50} values for MPP^+ and metformin (Lechner et al., 2016; Martinez-Guerrero et al., 2016). On the other hand, IC_{50} values for MPP^+ showed a tendency to be greater than those for metformin in efflux assays. Still, 10 out of the 12 compounds showed differences within 4-fold (Figure. 4B). The mechanism underlying the different substrate-dependencies in either uptake or efflux directions is not fully understood yet. Although this study carefully designed the efflux assays, this study cannot exclude the possibility that inhibitors interact with MATE1 from inside of the cells or inhibiting the intracellular binding or lysosomal trapping. Since the efflux

DMD Fast Forward. Published on December 1, 2020 as DOI: 10.1124/dmd.120.000136
This article has not been copyedited and formatted. The final version may differ from this version.

clearance was calculated using the total concentrations, this parameter is theoretically comprised of the intrinsic efflux clearance and intracellular unbound fraction. Even during the short incubation time of 0.25 min, the inhibitors can distribute to the cells depending on their passive permeability, participate in MATE1 inhibition, and modify the intracellular binding and lysosomal trapping. And this fact therefore indicates difficulties in both efflux and uptake inhibition studies to discriminate MATE1 inhibition from extracellular space from that from intracellular space completely as far as the non-polarized cells are used as host cells. Yet from the view point of preferring a conservative approach to assess DDI in order to mitigate any risk for patients, we believe that the uptake assay using metformin as the in vitro probe substrate offers the best condition to determine IC_{50} values of investigational drugs as inhibitors of MATE1.

We checked the impact of IC_{50} differences between uptake and efflux direction on predictions of MATE1-mediated clinical DDI risk using IC_{50} values based on metformin as a substrate. The DDI risk assessment according to the most conservative cut-off criteria ($I_{max,u}/IC_{50} > 0.02$) from the latest DDI guidelines from health authorities (MHLW., 2018) provided comparable results between uptake and efflux assays for all compounds. The assessment returned correct predictions of the AUC increase for 9 of the 10 drugs using the $I_{max,u}/ IC_{50}$ approach (Table 1), with the only exception of famotidine. The calculated $I_{max,u}/ IC_{50}$ values were 1.10 in the uptake direction and 0.322 in the efflux direction for famotidine, which are higher than the regulatory cutoff of 0.02; nevertheless, famotidine rather increased CL_R of metformin which was considered a result of modification of other sites by famotidine, such as urine pH modification and inhibition of reabsorption (Hibma et al., 2016). The unbound concentrations of MATE1 inhibitors in the plasma empirically seem to work as surrogates of those inside and/or lumen of the proximal tubules from where the inhibitors can address to MATE1. For instance, the quantitative analysis of dose dependent effect of

DMD Fast Forward. Published on December 1, 2020 as DOI: 10.1124/dmd.120.000136
This article has not been copyedited and formatted. The final version may differ from this version.

pyrimethamine on the renal clearance of metformin yielded apparent IC_{50} values defined from its plasma concentrations comparable with the corresponding in vitro IC_{50} values (Miyake et al., 2020). It remains a challenge to estimate the clinically relevant unbound concentrations of MATE1 inhibitors in the kidney for more precise prediction particularly when the transporters could concentrate or actively remove inhibitors inside the cells.

Efflux clearances of MPP^+ and metformin were 4-fold to 6.5-fold smaller compared to uptake clearances (MPP^+: 20 vs 130, metformin: 14 vs 55 μL/min/mg), although the same NH_4Cl concentration (20 mM) was used. Since efflux clearance was based on the total intracellular concentration, and thus different unbound intracellular concentrations might account for the discrepancy. We further speculate that a difference in the delta proton concentration between the outside and the inside of the cells might be one underlying mechanism. Considering that acute exposure to 20 mM NH_4Cl increased intracellular pH to 8.0 when the initial intracellular pH was 7.0 in another experiment (data not shown), the intracellular pH in the efflux assay in which the initial intracellular pH was 7.4 was estimated to be about 8.4, although a pH greater than 8.0 could not be measured due to a limitation of the method. In theory, the proton concentration in the efflux direction is 40 nM in the buffer (pH 7.4) and 4-10 nM within the cells (assuming the intracellular pH is 8.0-8.4), whereas the proton concentration in the uptake direction is 400 nM (pH 6.4) inside the cells and 40 nM in buffer (pH 7.4). Although the relative difference between extracellular and intracellular pH value is about one in both assay conditions, the absolute values of H^+ concentrations however differ almost 10-fold. This might affect the duration of initial velocities for uptake and efflux, and may have caused an underestimation of efflux clearance under the current conditions.

We compared IC_{50} values of 12 MATE1 inhibitors, in both uptake and efflux directions. The IC_{50} values obtained from uptake assay had a low propensity to generate different IC_{50} values as those obtained from efflux assay as long as metformin was used as the in vitro probe

DMD Fast Forward. Published on December 1, 2020 as DOI: 10.1124/dmd.120.000136
This article has not been copyedited and formatted. The final version may differ from this version.

substrate Moreover, the predictions of clinical inhibition of MATE1 using the $I_{max,u}/IC_{50}$ approach according to the most current regulatory guidance provided accurate predictions of AUC increases for 9 of the 10 inhibitors. The new assay tools, which can evaluate the MATE1 inhibitions separately from outside and from inside of the cells, may be expected to produce more physiologically relevant IC_{50} values. From the view point of drug development in pharmaceutical industries, together with our previous study (Lechner et al., 2016), we recommend the uptake assay using metformin as an in vitro probe substrate to determine IC_{50} values of new chemical entities for DDI risk assessment.

DMD Fast Forward. Published on December 1, 2020 as DOI: 10.1124/dmd.120.000136
This article has not been copyedited and formatted. The final version may differ from this version.

9. Acknowledgments

The excellent technical assistance of Saki Ichimura, and Michiru Miyake in performing the in vitro experiments at Nippon Boehringer Ingelheim is gratefully acknowledged. We also thank Dr. Caroline Maclean at Nippon Boehringer Ingelheim, Drs. Mitchell E. Taub and Stephanie Piekos at Boehringer Ingelheim Pharmaceuticals for editing a draft of this manuscript.

DMD Fast Forward. Published on December 1, 2020 as DOI: 10.1124/dmd.120.000136
This article has not been copyedited and formatted. The final version may differ from this version.

10. Authorship contributions

Participated in research design: Saito, Ishiguro, Takatani, Bister and Kusuhara

Conducted experiments: Saito, Takatani, Ichimura, and Miyake

Performed data analysis: Saito, Takatani, and Kusuhara

Wrote or contributed to the writing of the manuscript: Saito, Ishiguro, and Kusuhara

11. References

Becker ML, Visser LE, van Schaik RH, Hofman A, Uitterlinden AG, and Stricker BH (2009) Genetic variation in the multidrug and toxin extrusion 1 transporter protein influences the glucose-lowering effect of metformin in patients with diabetes: a preliminary study. *Diabetes* **58:**745-749.

Chu X, Bleasby K, Chan GH, Nunes I, and Evers R (2016) The Complexities of Interpreting Reversible Elevated Serum Creatinine Levels in Drug Development: Does a Correlation with Inhibition of Renal Transporters Exist? *Drug Metab Dispos* **44:**1498-1509.

Dangprapai Y and Wright SH (2011) Interaction of H^+ with the extracellular and intracellular aspects of hMATE1. *Am J Physiol Renal Physiol* **301:**F520-528.

European Medicines Agency (2012) EMA guideline on the investigation of drug interactions. 2012. Final CPMP/EWP/560/95.

U.S. Food, Drug Administration (2020) In vitro drug interaction studies-cytochrome P450 enzyme- and transporter-mediated drug interactions.

Gillen CM and Forbush B, 3rd (1999) Functional interaction of the K-Cl cotransporter (KCC1) with the Na-K-Cl cotransporter in HEK-293 cells. *Am J Physiol* **276:**C328-336.

He X, Szewczyk P, Karyakin A, Evin M, Hong WX, Zhang Q, and Chang G (2010) Structure of a cation-bound multidrug and toxic compound extrusion transporter. *Nature* **467:**991-994.

Hibma JE, Zur AA, Castro RA, Wittwer MB, Keizer RJ, Yee SW, Goswami S, Stocker SL, Zhang X, Huang Y, Brett CM, Savic RM, and Giacomini KM (2016) The Effect of Famotidine, a MATE1-Selective Inhibitor, on the Pharmacokinetics and Pharmacodynamics of Metformin. *Clin Pharmacokinet* **55:**711-721.

Ito S, Kusuhara H, Yokochi M, Toyoshima J, Inoue K, Yuasa H, and Sugiyama Y (2012) Competitive inhibition of the luminal efflux by multidrug and toxin extrusions, but not basolateral uptake by organic cation transporter 2, is the likely mechanism underlying the pharmacokinetic drug-drug interactions caused by cimetidine in the kidney. *J Pharmacol Exp Ther* **340:**393-403.

Ivanyuk A, Livio F, Biollaz J, and Buclin T (2017) Renal Drug Transporters and Drug Interactions. *Clin Pharmacokinet* **56:**825-892.

Kusuhara H, Ito S, Kumagai Y, Jiang M, Shiroshita T, Moriyama Y, Inoue K, Yuasa H, and Sugiyama Y (2011) Effects of a MATE protein inhibitor, pyrimethamine, on the renal elimination of metformin at oral microdose and at therapeutic dose in healthy subjects. *Clin Pharmacol Ther* **89:**837-844.

Lechner C, Ishiguro N, Fukuhara A, Shimizu H, Ohtsu N, Takatani M, Nishiyama K, Washio I, Yamamura N, and Kusuhara H (2016) Impact of Experimental Conditions on the Evaluation of Interactions between Multidrug and Toxin Extrusion Proteins and Candidate Drugs. *Drug Metab Dispos* **44:**1381-1389.

Li Q, Guo D, Dong Z, Zhang W, Zhang L, Huang SM, Polli JE, and Shu Y (2013) Ondansetron can enhance cisplatin-induced nephrotoxicity via inhibition of multiple toxin and extrusion proteins (MATEs). *Toxicol Appl Pharmacol* **273:**100-109.

Lowry OH, Rosebrough NJ, Farr AL, and Randall RJ (1951) Protein measurement with the Folin phenol reagent. *J Biol Chem* **193:**265-275.

Lu M, Radchenko M, Symersky J, Nie R, and Guo Y (2013) Structural insights into H+-coupled multidrug extrusion by a MATE transporter. *Nat Struct Mol Biol* **20:**1310-1317.

Martínez-Guerrero LJ, Evans KK, Dantzler WH, and Wright SH (2016) The multidrug transporter MATE1 sequesters OCs within an intracellular compartment that has no

influence on OC secretion in renal proximal tubules. *Am J Physiol Renal Physiol* 310:F57-67.

Martinez-Guerrero LJ, Morales M, Ekins S, and Wright SH (2016) Lack of Influence of Substrate on Ligand Interaction with the Human Multidrug and Toxin Extruder, MATE1. *Mol Pharmacol* **90:**254-264.

Ministry of Health, Labor and Welfare (2018) Guideline on drug interaction for drug development and appropriate provision of information.

Miyake T, Kimoto E, Luo L, Mathialagan S, Horlbogen LM, Ramanathan R, Wood LS, Johnson JG, Le VH, Vourvahis M, Rodrigues AD, Muto C, Furihata K, Sugiyama Y, and Kusuhara H (2020) Identification of Appropriate Endogenous Biomarker for Risk Assessment of Multidrug and Toxin Extrusion Protein-Mediated Drug-Drug Interactions in Healthy Volunteers. *Clin Pharmacol Ther*.

Miyauchi H, Moriyama S, Kusakizako T, Kumazaki K, Nakane T, Yamashita K, Hirata K, Dohmae N, Nishizawa T, Ito K, Miyaji T, Moriyama Y, Ishitani R, and Nureki O (2017) Structural basis for xenobiotic extrusion by eukaryotic MATE transporter. *Nat Commun* **8:**1633.

Motohashi H and Inui K (2013) Multidrug and toxin extrusion family SLC47: physiological, pharmacokinetic and toxicokinetic importance of MATE1 and MATE2-K. *Mol Aspects Med* **34:**661-668.

Nakada T, Kudo T, Kume T, Kusuhara H, and Ito K (2019) Estimation of changes in serum creatinine and creatinine clearance caused by renal transporter inhibition in healthy subjects. *Drug Metab Pharmacokinet* **34:**233-238.

Prasad B, Johnson K, Billington S, Lee C, Chung GW, Brown CD, Kelly EJ, Himmelfarb J, and Unadkat JD (2016) Abundance of Drug Transporters in the Human Kidney Cortex

as Quantified by Quantitative Targeted Proteomics. *Drug Metab Dispos* **44:**1920-1924.

Stocker SL, Morrissey KM, Yee SW, Castro RA, Xu L, Dahlin A, Ramirez AH, Roden DM, Wilke RA, McCarty CA, Davis RL, Brett CM, and Giacomini KM (2013) The effect of novel promoter variants in MATE1 and MATE2 on the pharmacokinetics and pharmacodynamics of metformin. *Clin Pharmacol Ther* **93:**186-194.

Tanaka Y, Hipolito CJ, Maturana AD, Ito K, Kuroda T, Higuchi T, Katoh T, Kato HE, Hattori M, Kumazaki K, Tsukazaki T, Ishitani R, Suga H, and Nureki O (2013) Structural basis for the drug extrusion mechanism by a MATE multidrug transporter. *Nature* **496:**247-251.

Terada T and Inui K (2008) Physiological and pharmacokinetic roles of H+/organic cation antiporters (MATE/SLC47A). *Biochem Pharmacol* **75:**1689-1696.

Thomas JA, Buchsbaum RN, Zimniak A, and Racker E (1979) Intracellular pH measurements in Ehrlich ascites tumor cells utilizing spectroscopic probes generated in situ. *Biochemistry* **18:**2210-2218.

Tsuda M, Terada T, Ueba M, Sato T, Masuda S, Katsura T, and Inui K (2009) Involvement of human multidrug and toxin extrusion 1 in the drug interaction between cimetidine and metformin in renal epithelial cells. *J Pharmacol Exp Ther* **329:**185-191.

Yonezawa A and Inui K (2011a) Importance of the multidrug and toxin extrusion MATE/SLC47A family to pharmacokinetics, pharmacodynamics/toxicodynamics and pharmacogenomics. *Br J Pharmacol* **164:**1817-1825.

Yonezawa A and Inui K (2011b) Organic cation transporter OCT/SLC22A and H(+)/organic cation antiporter MATE/SLC47A are key molecules for nephrotoxicity of platinum agents. *Biochem Pharmacol* **81:**563-568.

DMD Fast Forward. Published on December 1, 2020 as DOI: 10.1124/dmd.120.000136
This article has not been copyedited and formatted. The final version may differ from this version.

12. Footnote

This study was supported by Nippon Boehringer Ingelheim Co., Ltd.

DMD Fast Forward. Published on December 1, 2020 as DOI: 10.1124/dmd.120.000136
This article has not been copyedited and formatted. The final version may differ from this version.

13. Figure Legends

Figure 1 Time profiles of intracellular [^{3}H]MPP$^+$ (A) and [^{3}H]metformin (B) in MATE1-expressing HEK293 cells.

After pre-loading [^{3}H]MPP$^+$ (0.01 μM) and [^{3}H]metformin (0.1 μM) for 10 min, efflux was initiated in 20 mM NH_4Cl buffer at pH 7.4 and the remaining concentrations of substrates in the cells were measured. Each point represents the mean value ± S.D. (n = 3).

Figure 2 Inhibitory effect of various compounds on the efflux of [^{3}H]MPP$^+$.

Efflux of [^{3}H]MPP$^+$ was determined in the absence and presence of indicated inhibitors in 20 mM NH_4Cl buffer at pH 7.4 for 0.25 min. Each point represents the mean value ± S.E. (n = 3).

Figure 3 Inhibitory effect of various compounds on the efflux of [^{3}H]metformin.

Efflux of [^{3}H]metformin was determined in the absence and presence of indicated inhibitors in 20 mM NH_4Cl buffer at pH 7.4 for 0.25 min. Each point represents the mean value ± S.E. (n = 3).

Figure 4 Comparison of IC_{50} values from uptake and efflux direction using MPP$^+$ and metformin as a probe substrates.

IC_{50} values were determined by nonlinear regression analysis and compared between different transport directions (uptake and efflux, A), and different substrates (MPP$^+$ and metformin, B). IC_{50} values of cephalexin in the efflux direction were not plotted due to no observed inhibition at the highest concentration (10 mM). The black line represents the line of unity and the dotted lines represent 4-fold errors.

14. TABLES

Table1: DDI risk assessment based on IC_{50} values from uptake/efflux directions and plasma unbound C_{max} ($C_{max,u}$).

Inhibitor	IC_{50} (μM), MATE1				$C_{max,u}$	Metformin AUC change	$C_{max,u}/IC_{50,\ Metfromin}$	
	MPP^+		Metformin		(μM)	(%)		
	Uptake	Efflux	Uptake	Efflux			Uptake	Efflux
Pyrimethamine*	0.492 ± 0.039	1.19 ± 0.061	0.313 ± 0.052	0.502 ± 0.058	0.298	35.3-170	0.95	0.59
Cimetidine*	4.43 ± 0.05	43.8 ± 0.13	2.56 ± 0.04	6.12 ± 0.077	7.74	46.2-54.2	3.0	1.3
Trimethoprim*	8.16 ± 0.06	84.5 ± 0.087	4.13 ± 0.09	11.3 ± 0.13	8.88	21.5-68.6	2.2	0.79
Quinidine*	6.77 ± 0.08	15.5 ± 0.094	5.82 ± 0.06	5.00 ± 0.12	1.34	no data	0.23	0.27
Ondansetron*	0.797 ± 0.025	0.935 ± 0.15	0.436 ± 0.083	0.624 ± 0.19	0.0471	21	0.11	0.076
Famotidine*	1.670 ± 0.03	10.7 ± 0.12	0.905 ± 0.046	3.11 ± 0.12	1	2.7	1.1	0.32
Dolutegravir	7.12 ± 0.085	23.8 ± 0.23	3.04 ± 0.086	9.07 ± 0.30	0.180	78.9-145	0.059	0.020
Vandetanib	3.36 ± 0.06	3.52 ± 0.17	2.39 ± 0.034	1.60 ± 0.13	0.102	73.3	0.043	0.064
Cephalexin	2614 ± 0.02	>10,000	2110 ± 0.043	>10,000	69.3	23.9	0.033	N.A.
Ranolazine	88.1 ± 0.043	111 ± 0.092	48.7 ± 0.061	66.3 ± 0.31	1.85	38.5-83	0.038	0.028
Lansoprazole	60.1 ± 0.049	148 ± 0.22	44.0 ± 0.056	66.5 ± 0.24	0.0883	11.8	0.0020	0.0013
Cobicistat	5.29 ± 0.087	12.2 ± 0.11	2.75 ± 0.083	5.27 ± 0.23	0.054	no data	0.020	0.010

IC_{50} values were estimated by nonlinear regression analysis and are given as mean ±S.D.

N.A., not applicable

*: IC_{50} values obtained by uptake assay were from Lechner et al. (2016)

Figure 1

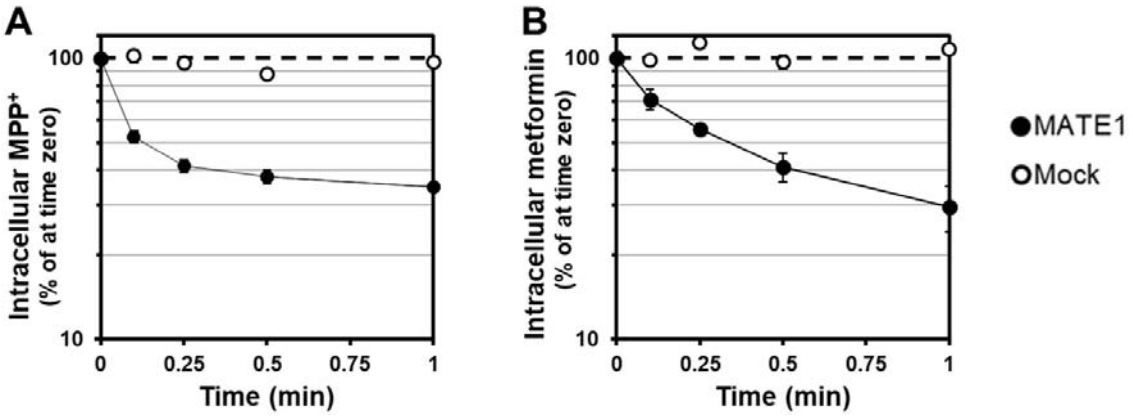

Figure 2

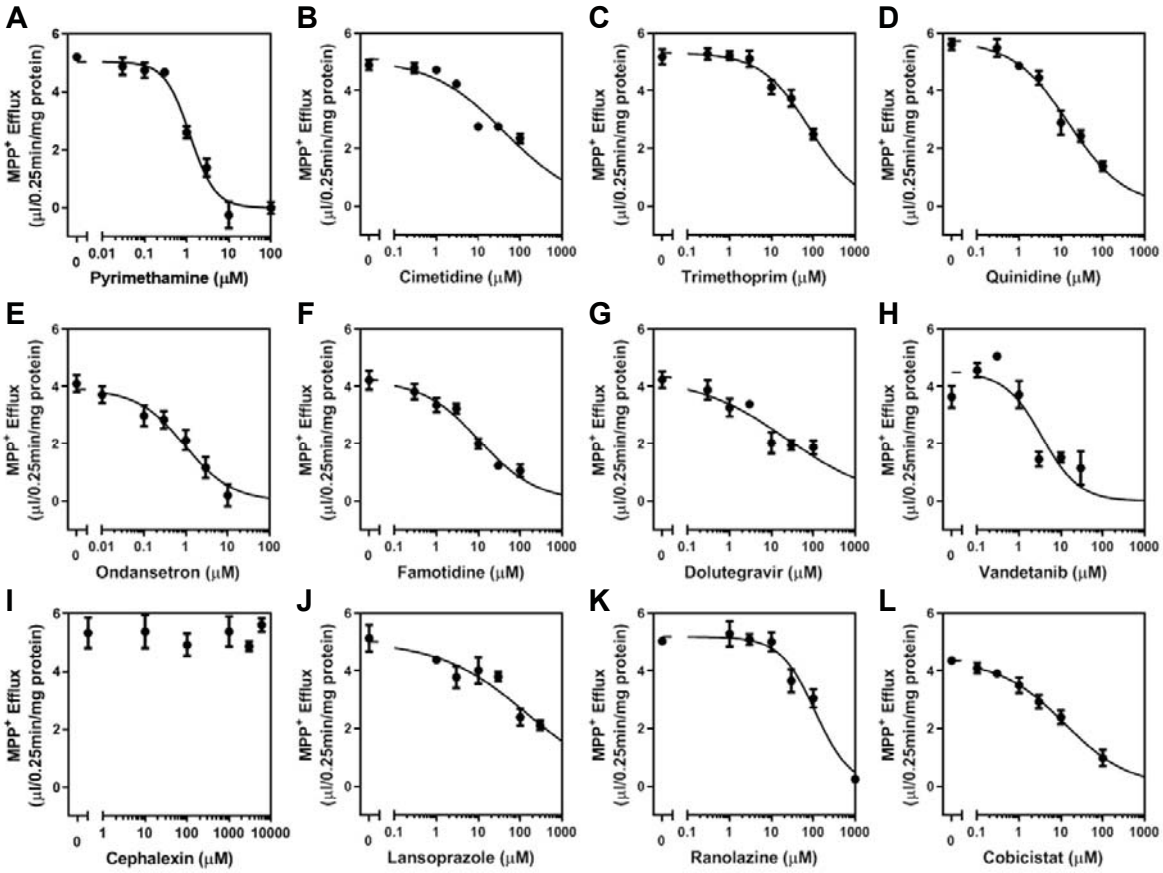

Figure 3

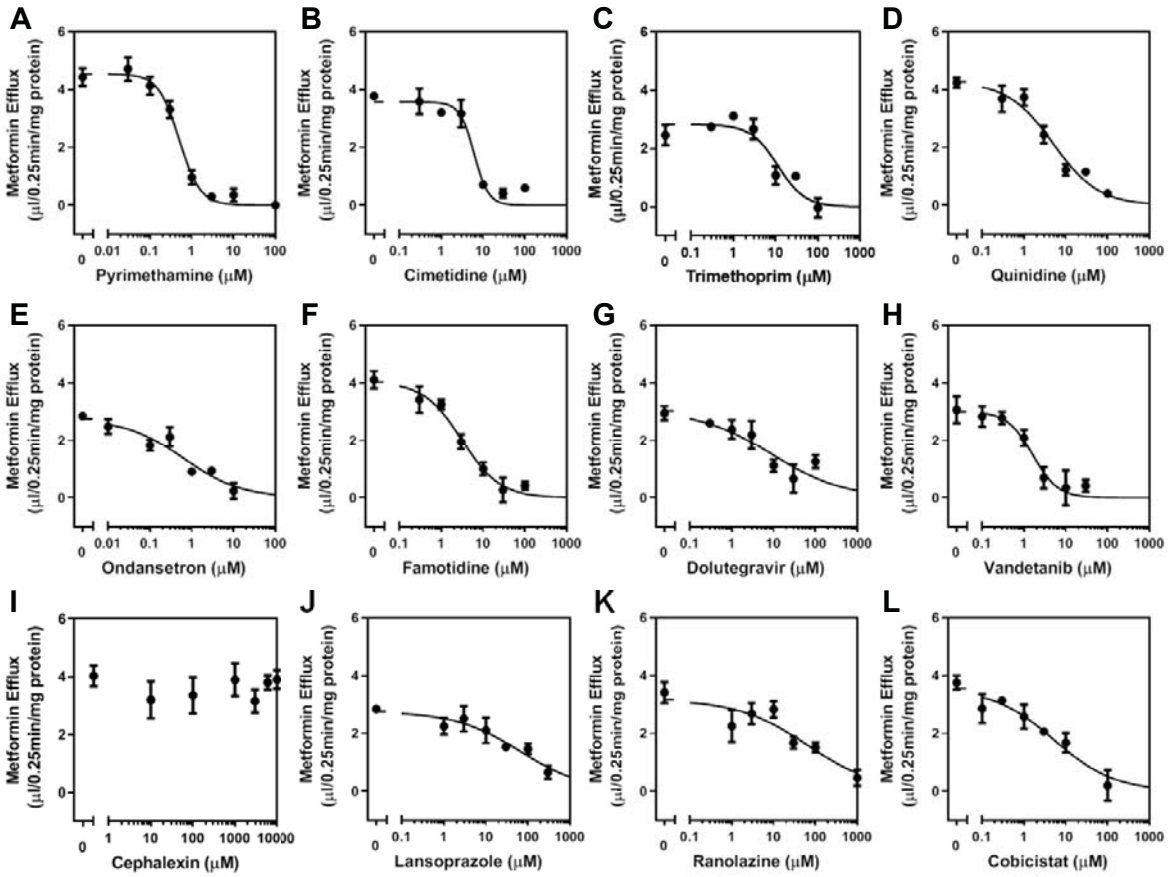

Figure 4